Shallow donors in magnetic fields in zinc-blende semiconductors. II. Magneto-optical study of InSb under hydrostatic pressure

Louis-Claude Brunel, Serge Huant, Michał Baj,* and Witold Trzeciakowski†

Service National des Champs Intenses, Centre National de la Recherche Scientifique, Boîte Postale 166X, F-38042 Grenoble Cédex, France

(Received 3 September 1985)

Four intraimpurity transitions between the shallow states of residual donors were studied as a function of a high magnetic field up to 19 T and of a hydrostatic pressure up to 1.1 GPa in nominally undoped n-type InSb samples. The measurements were performed mainly with the photoconductivity technique in the 5—30-cm^{-1} spectral region using a far-infrared-laser system. Good quantitative agreement with the multiband approach proposed by Trzeciakowski *et al.* (preceding paper) is obtained at zero pressure as well as under pressure (provided that the pressure variation of the dielectric constant is taken into account) in a wide range of high effective magnetic fields $10<\gamma<130$ [$\gamma=\hbar\omega_c/(2\ \mathrm{Ry}^*)$]. The study of the chemical shifts for the observed donors allows for the determination of the matrix elements of the localized parts of the impurity potentials $(S\,|\,V_{\mathrm{loc}}\,|\,S)$. For the deepest of the donors (donor A) this matrix element increases significantly with pressure. Moreover, at pressures around 0.65 GPa, the ground state of the donor A anticrosses with another level of the same impurity center, resonant with the conduction band in the absence of field and pressure. Detailed study of the anticrossing within a simple two-level model shows that the "resonant" level can be treated as deep, i.e., essentially bound by V_{loc}, while the Coulomb potential shifts its position by about 0.1 eV.

I. INTRODUCTION

Owing to the low electronic effective-mass ($m^*\sim0.0135m_0$) and the relatively high dielectric constant ($\epsilon_0\sim17$) of the narrow-gap semiconductor InSb ($E_g\sim235$ meV), the influence of the magnetic field B on shallow donor states in InSb is much greater than in most other hydrogeniclike systems. Even in the purest available samples of InSb the donor states cannot be observed without sufficiently strong magnetic field, because of the large Bohr radius ($a_B^*\sim600$ Å) which results in a strong overlap of the zero-field donor wave functions. The magnetic field effect on shallow donors can be measured by the dimensionless parameter $\gamma=\hbar\omega_c/(2\ \mathrm{Ry}^*)$ which is proportional to ϵ_0^2B/m^{*2} (all symbols are those of Ref. 1, hereafter denoted as I). In a field of 20 T which is commonly reached today in high-field facilities, we have $\gamma=130$ in InSb (high-field regime) but only 3 in GaAs (intermediate field) and almost 10^{-4} for the hydrogen atom (low-field regime). This implies the necessity to use a multiband approach (see I) for the description of donor states in a magnetic field in InSb.

Since the energy gap strongly depends on pressure ($dEg/dP\sim140$ meV/GPa), high hydrostatic pressure allows to monitor the electronic properties of the material and also to vary γ at a given B mainly through the dependence upon pressure of m^* (e.g., the pressure of 1.8 GPa doubles m^*). This gives an opportunity to judge between various theories dealing with shallow donor states in high magnetic fields (see I and references therein) in a wide range of γ.

The first magneto-optical studies of shallow donors in InSb performed in fields up to 10 T by Kaplan[2–4] suggested that for the proper description of the experimental results, both the band nonparabolicity and the chemical shifts (CS) of the impurity ground level should be taken into account. Cooke[5] and Kaplan[6] extended the study in the 10—15-T range and discussed the CS and the chemical nature of the four residual donors they found in all the samples they studied. Very recently, the identification of the donors was investigated more precisely by Kuchar *et al.*[7] Magneto-optical experiments were performed under hydrostatic pressure by Davidson *et al.*[8] and Wasilewski *et al.*[9,10] The latter authors observed at pressures around 650 MPa an interesting phenomenon of anticrossing of the lowest lying of the shallow levels with another level belonging to the same center (previously reported in transport measurements[11]) which they believed to be associated with the subsidiary L minimum of the conduction band. In recent Hall-effect measurements under pressure,[12] a decrease of the carrier concentration in sufficiently doped n-type InSb samples was found to be due to the trapping of the carriers onto that latter impurity level at pressures at which it was still resonant with the conduction band. Pressure experiments are generally known to be very useful for the detection of impurity levels which are initially resonant with the energy continuum of the host material and/or which are associated with a subsidiary minimum of the band.[13] In particular, the above-mentioned level anticrossing can be observed only under high pressure which brings both levels into the same energy region. Moreover, the study of the pressure coefficients of the levels enables to distinguish between shallow and deep states[14] and, in the case of shallow states, to specify the minimum they originate from.

In this paper we report on the systematic study in the

5–30 cm^{-1} energy range of the magneto-optical transitions between bound impurity states in nominally undoped n-type InSb under hydrostatic pressures up to 1.1 GPa.[15] As the nonparabolic effects become substantial in the high-field region (see I) we have extended the magnetic field range up to 19 T. In order to increase the accuracy of the measurements we used an optically-pumped (CO_2 laser) far-infrared laser (FIRL) instead of the Fourier-transform spectrometer (FTS) used in most of the previous studies. It yields a better signal-to-noise ratio which also enabled us to study weak transitions not observed before. In particular, the transitions between the excited states are of special interest as they are almost not affected by the central-cell potential V_{loc} (no CS), and thus can be directly compared with theory. The energies of all the observed transitions were compared with calculations based on nonparabolic theories. The transitions involving the ground state enabled us to determine the matrix elements of V_{loc}. Our measurements allowed for a more precise investigation of the level anticrossing[8–10] and its pressure and magnetic field dependence. One reason is that we used a more powerful light source and thus the transitions were measurable in a much wider energy range than in FTS experiments. Another reason is that for the transition energies rapidly varying with the field (as in the case of the anticrossing branches) the determination of the peak position is much more precise if one sweeps the magnetic field (FIRL) rather than changes the energy (FTS).

The paper is organized as follows. In Sec. II, the experimental setup is described. We present our experimental results in Sec. III; their interpretation appears in Sec. IV, and the conclusions in Sec. V.

II. EXPERIMENT

We used n-type InSb samples prepared from nominally undoped material with a free carrier concentration of 1.2×10^{14} cm^{-3} and a mobility of 5.5×10^{5} $cm^2/V/sec.$ at 77 K.

All the measurements were performed at 4.2 K. Most of the results were obtained using the photoconductivity technique which provides a very sensitive tool for the investigation of intraimpurity transitions in pure materials.[2] For these photoconductivity measurements the samples were thin platelets of thickness close to 50 μm, the irradiated area was 1×3 mm^2. After etching in a bromine-methanol solution, four contacts were made by soldering thin copper wires with small indium dots. We recorded the photoconductivity spectra with either a constant current through the sample or with a constant voltage applied to the sample; both techniques appear complementary especially at low magnetic field when the resistance of the sample increases rapidly with magnetic field.[16] In either case, we always worked in the Ohmic region of the current density electric field characteristics of the sample. We also performed some absorption measurements with a 2.5-mm-thick sample using an external Ge bolometer.[17] In both photoconductivity and absorption measurements the signal was analyzed by a two-phase lock-in detection at a frequency of typically 30 Hz. In our experiments, we used an optically pumped (CO_2 laser) FIRL with nine different gases in order to obtain about 40 lines between 339 μm ($E=29.50$ cm^{-1}) and 1 899 μm ($E=5.27$ cm^{-1}). Therefore, the measurements were done at fixed wavelengths and the spectra were recorded by sweeping the magnetic field provided by a 10 MW bitter coil. Fields of up to 19 T were applied parallel to the {111} crystallographic direction and to the wave vector of the incident light (Faraday configuration). However, some longitudinal components (Voigt configuration) may arise because of multireflections in the wave guide or in the pressure cell. The light was unpolarized.

High hydrostatic pressures up to 1.1 GPa were obtained in a Be-Cu liquid pressure cell, supplied with an optical sapphire window[18] and containing, as a pressure transmitting medium, a mixture of light hydrocarbons chosen to guarantee the hydrostaticity of the pressure. We measured the pressure with an accuracy of about 1% using a semiconducting gauge.[19]

III. EXPERIMENTAL RESULTS

In the following (Figs. 1–5), we show a few examples of FIRL photoconductivity spectra which reveal some features of the experimental technique we used and some physical phenomena which will be discussed later on.

Figure 1 shows typical photoconductivity spectra which exhibit the (000)→(0$\bar{1}$0) transition at zero pressure for different FIRL lines. One can see up to four peaks, the

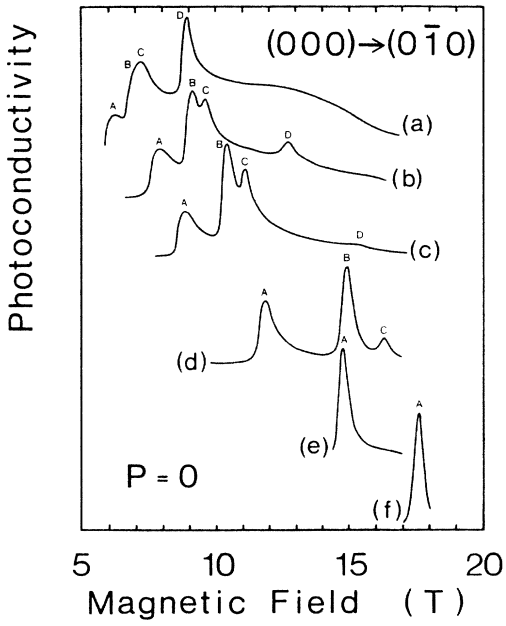

FIG. 1. Photoconductivity spectra (arbitrary units) of the (000)→(0$\bar{1}$0) transition recorded at zero pressure with various laser energies: (a), $E=10.38$ cm^{-1}; (b), $E=11.24$ cm^{-1}; (c), $E=11.72$ cm^{-1}; (d), $E=13.09$ cm^{-1}; (e), $E=14.31$ cm^{-1}; (f), $E=15.48$ cm^{-1}. Four residual donors(A through D) contribute to the transitions.

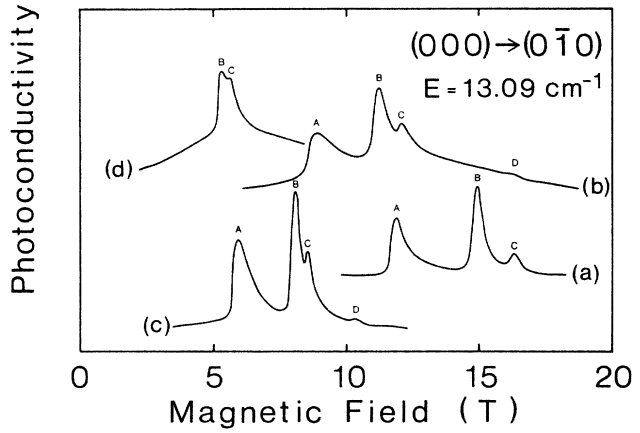

FIG. 2. Photoconductivity spectra (arbitrary units) of the (000)→(0$\bar{1}$0) transition at the laser energy $E=13.09$ cm^{-1} for various pressures: (a), $P=0$; (b), $P=0.265$ GPa; (c), $P=0.59$ GPa; (d), $P=1.1$ GPa.

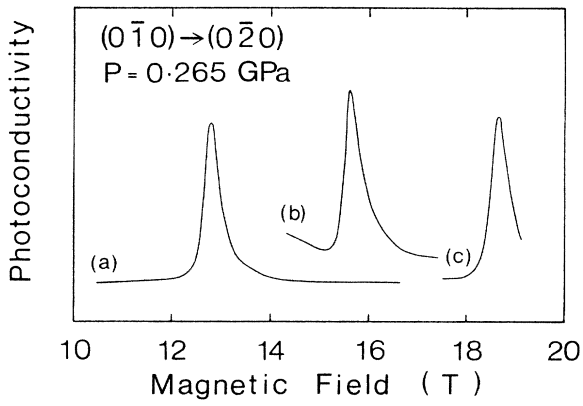

FIG. 4. Photoconductivity spectra (arbitrary units) of the (0$\bar{1}$0)→(0$\bar{2}$0) transition at a pressure of 0.265 GPa with various laser energies: (a), $E=5.27$ cm^{-1}; (b), $E=5.81$ cm^{-1}; (c), $E=6.20$ cm^{-1}.

higher the field the better the resolution. For the highest energies, the structure progressively goes outside the available field range. This structure is typical of the photothermal[2,20] excitation spectra of the four residual donors (labeled A,B,C, and D in order of decreasing binding energy) which are commonly observed in "pure" n-type InSb samples. The relative intensities of the four peaks in Fig. 1 strongly vary with the magnetic field (the spectra are to scale); this is essentially an artifact of the experimental method we used. Indeed, during the sweeping of the magnetic field which is necessary to record the spectra at fixed wavelengths, the resistance of the sample increases by up to 7 orders of magnitude at zero pressure because of the "magnetic freeze-out".[21] This change in resistance induces a drastic modification in the sensitivity of the photoconductivity technique. Furthermore, sweeping the magnetic field modifies, on one hand, the energies of all the impurity states and thus the efficiency of the photothermal effect[20] and, on the other hand, the population of these levels and thus the intensities of the transitions between them. For all the above reasons, it is not possible to compare the relative intensities of the photo-

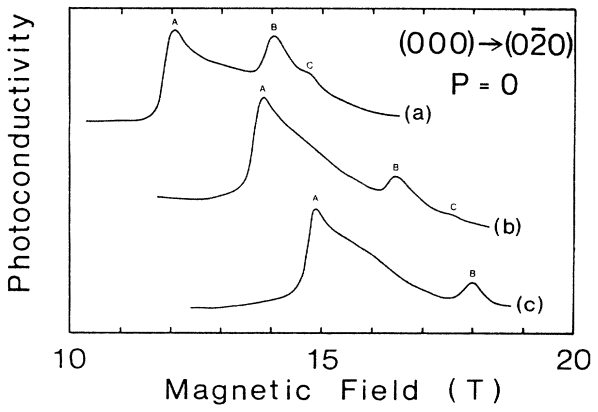

FIG. 3. Photoconductivity spectra (arbitrary units) of the (000)→(0$\bar{2}$0) transition at zero pressure with various laser energies: (a), $E=18.05$ cm^{-1}; (b), $E=19.12$ cm^{-1}; (c), $E=19.69$ cm^{-1}.

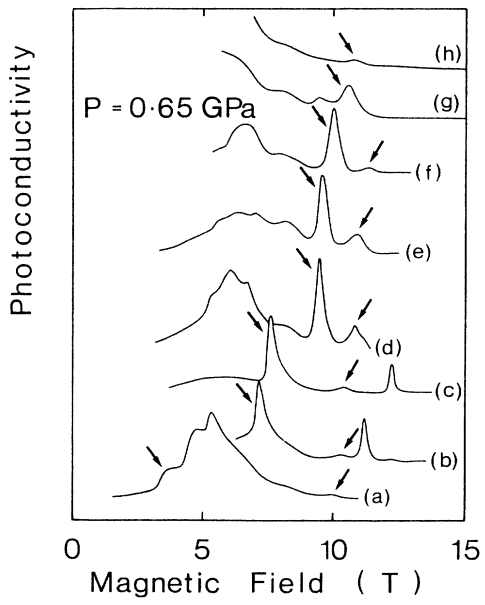

FIG. 5. Photoconductivity spectra (arbitrary units) revealing the anticrossing of the shallow (000) level of the donor A with the deep state of the same impurity. The anticrossing manifests itself on the transitions from these two levels to the (0$\bar{1}$0) excited state (marked with arrows). The remaining structures are due either to the transitions (000)→(0$\bar{1}$0) for donors B,C, and D [curves (a), (b), and (c) as shown in Fig. 1], or to the transitions (000)→(0$\bar{2}$0) [curves (d), (e), and (f) as shown on Fig. 3]. The laser energies are (a), $E=11.24$ cm^{-1}; (b), $E=14.70$ cm^{-1}; (c), $E=15.08$ cm^{-1}; (d), $E=17.24$ cm^{-1}; (e), $E=17.53$ cm^{-1}; (f), $E=18.05$ cm^{-1}; (g), $E=23.37$ cm^{-1}; (h), $E=24.63$ cm^{-1}.

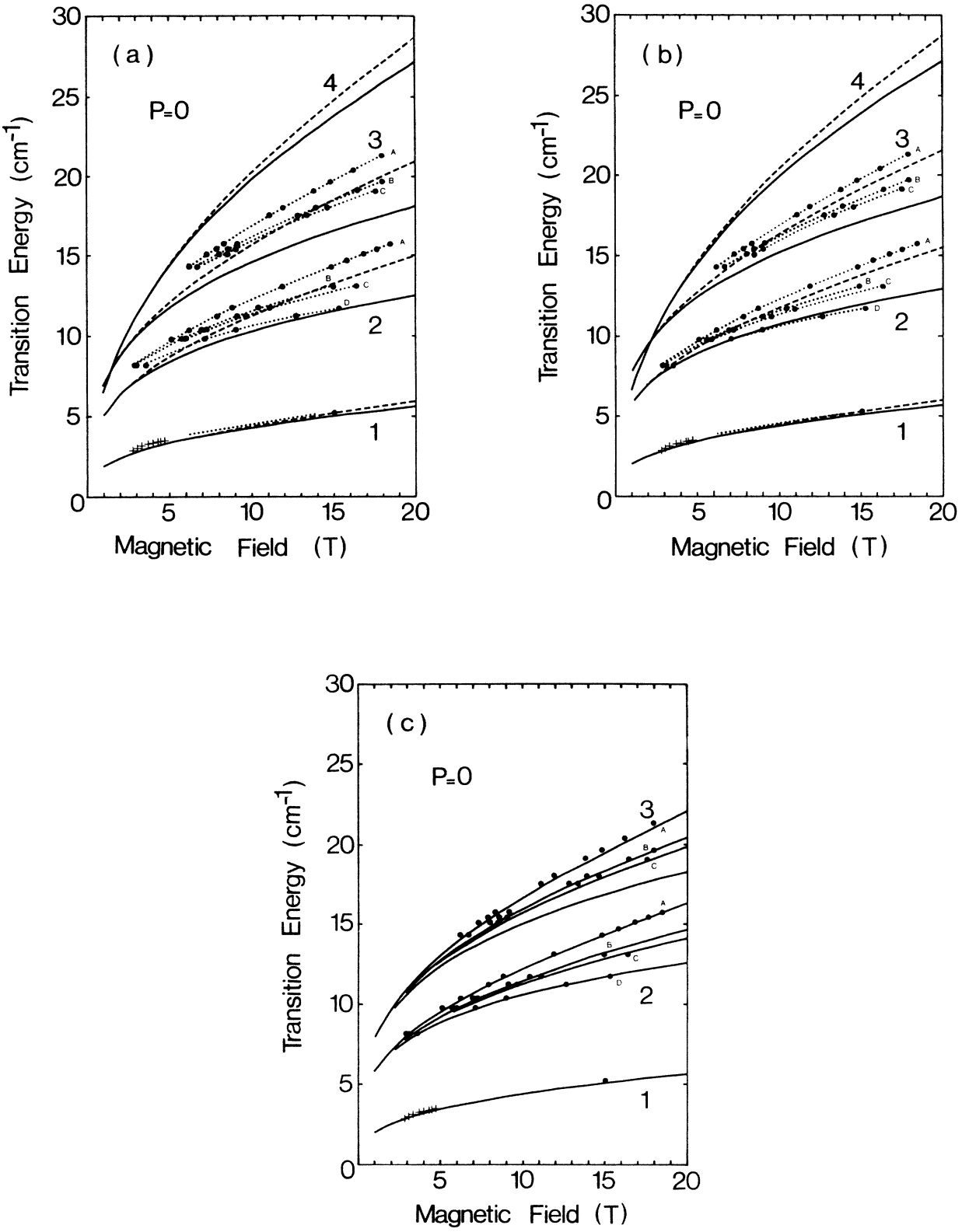

FIG. 6. Magnetic field dependence of the intradonor optical transitions measured at $P=0$: 1, $(0\bar{1}0)\rightarrow(0\bar{2}0)$; 2, $(000)\rightarrow(0\bar{1}0)$; 3, $(000)\rightarrow(0\bar{2}0)$; 4, $(0\bar{1}0)\rightarrow(0\bar{1}1)$. Crosses are the points taken from Ref. 23. Dotted lines are the experimental curves, the one for transition 1 obtained by subtraction of those for transitions 2 and 3. Solid and dashed lines are calculated according to TBHB and ZW models, respectively, (a) without the correction factors (see the text); (b) with the correction factors; (c) with both correction factors and chemical shifts taken into account (here only for the TBHB model).

conductivity peaks. The apparent asymmetry of the peaks in Fig. 1 (and also in Figs. 2–5) is mainly due to the rapid change of the sample resistance and to the slow variation of the transition energies with the magnetic field. It is, however, important that these inconveniences do not affect the field positions of the peaks which are still sufficiently sharp.[7] In a few cases, we checked that for the (000)→(0$\bar{1}$0) transition the spectra obtained in photoconductivity measurements (either with a constant current in the sample or a constant voltage applied to the sample) and the transmission measurements gave exactly the same peak positions.

Figure 2 shows the spectra of the same transition as on Fig. 1 recorded at a given wavelength but for four different pressures. The positions of the peaks are quite sensitive to the pressure and the peak corresponding to donor A disappears at the highest pressure due to the anticrossing described in Sec. IV. Figure 3 shows the spectra corresponding to the transition observed for the first time, identified unambiguously (see the next section) as (000)→(0$\bar{2}$0). It involves the ground impurity state and is therefore central-cell resolved. In most cases we did not observe it for the donor D. The absorption coefficient of this dipole-forbidden transition measured in transmission experiment was almost 10 times lower than that of the (000)→(0$\bar{1}$0) transition at the same field. The violation of the $\Delta M=0,\pm1$ selection rule must be due to some additional terms in the Hamiltonian, lowering its cylindrical

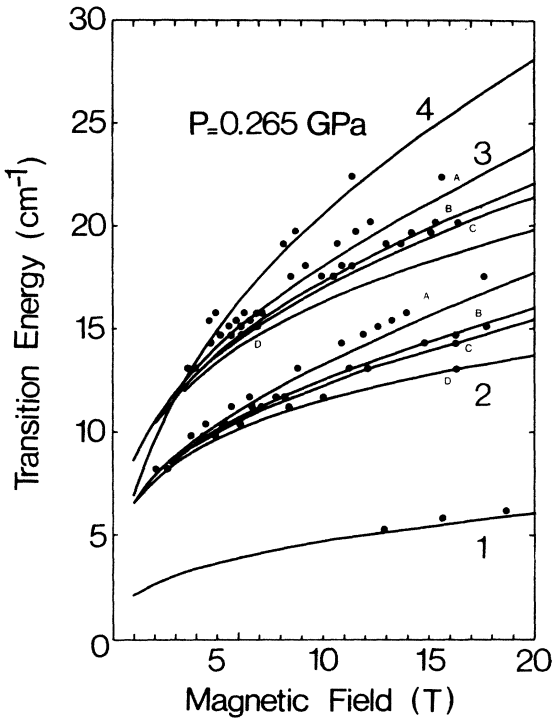

FIG. 7. The magnetic field dependence of the intradonor optical transitions (numbered as in Fig. 6) measured at $P=0.265$ GPa. Solid lines are calculated with both correction factors (see the text) and chemical shifts taken into account. Anomalous deepening of the donor A is already visible.

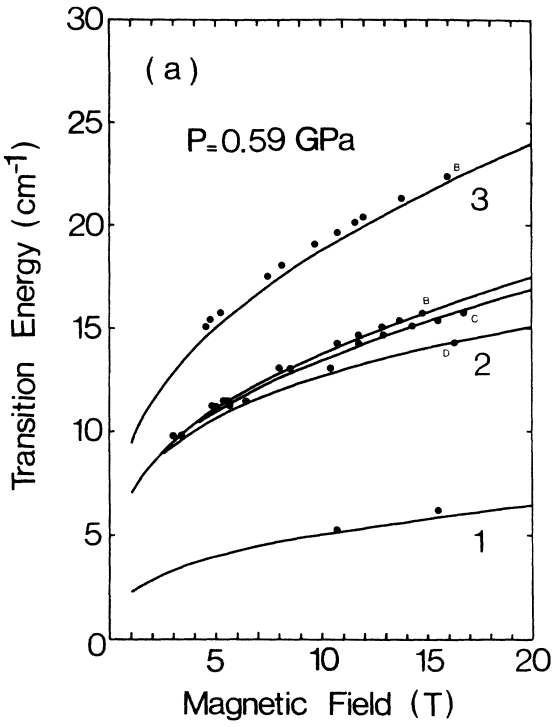

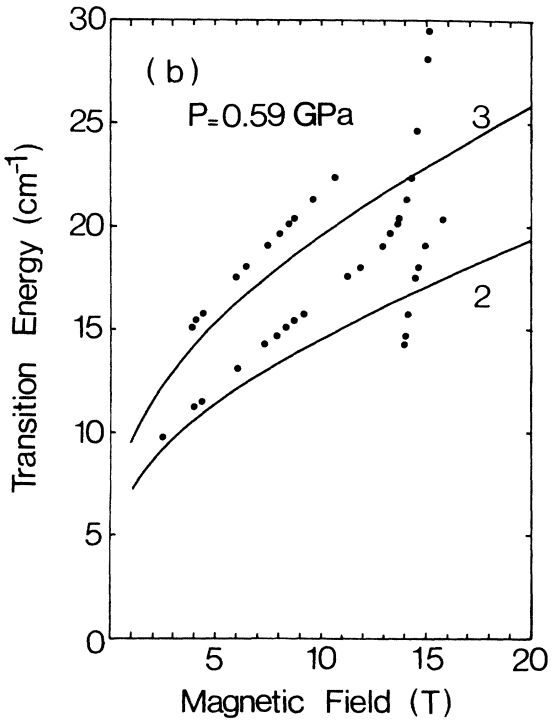

FIG. 8. The magnetic field dependence of the intradonor optical transitions (numbered as in Fig. 6) measured at $P=0.59$ GPa. Solid lines are calculated from the TBHB model with the correction factors and chemical shifts included: (a) donors B,C, and D; (b) donor A only. Both the interaction and the anomalous deepening of the donor A are clearly visible.

symmetry. Such terms may arise from warping or inversion asymmetry[22] or from the presence of random electric fields (originating from ionized impurities). The transition $(0\bar{1}0)\rightarrow(0\bar{2}0)$ shown in Fig. 4 (observed at $P=0$ by Blagosklonkaya *et al.*[23]) has no central-cell structure thus revealing no CS for the $(0\bar{1}0)$ state, possible within the nonparabolic theory (see I).

Figure 5 shows the example of the spectra for the $(000)\rightarrow(0\bar{1}0)$ transition measured at 650 MPa, revealing the "interaction" (anticrossing) of the shallow state (000) of the donor A with the deep state related to the same impurity center (see Sec. IV). The arrows in Fig. 5 point out the positions of the two anticrossing branches. For the sake of clarity the spectra of Fig. 5 were recorded with the constant current through the sample in the whole range of the magnetic field. However, to determine precisely the

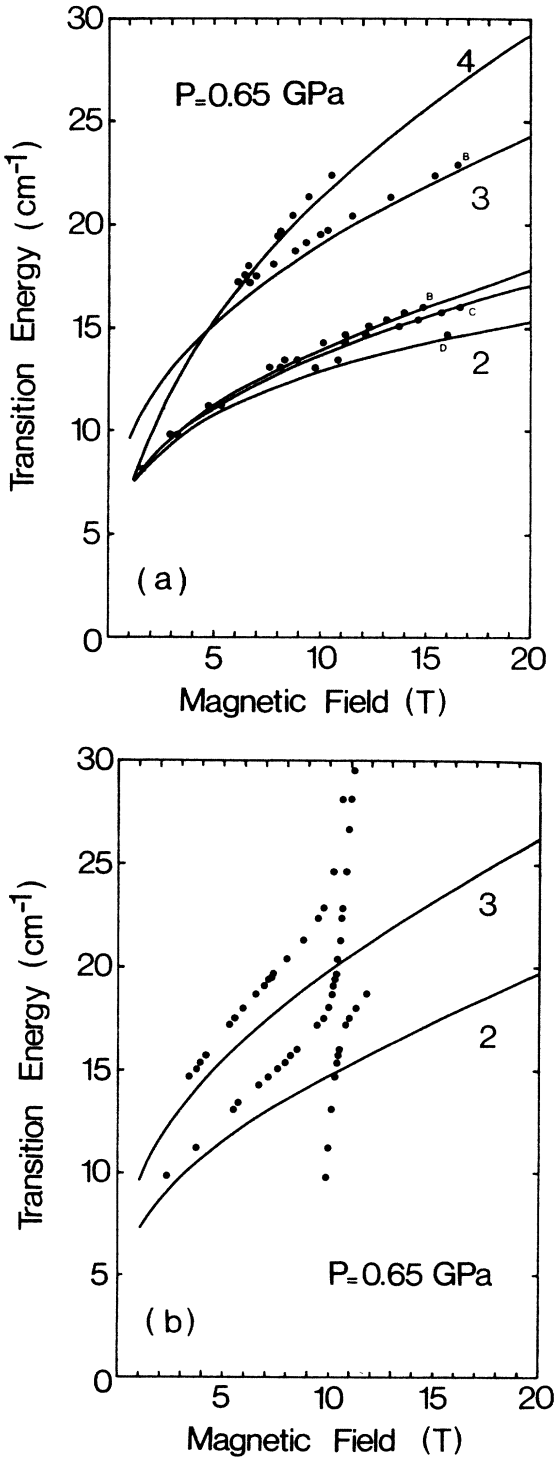

FIG. 9. Same as Fig. 8 but for $P=0.65$ GPa.

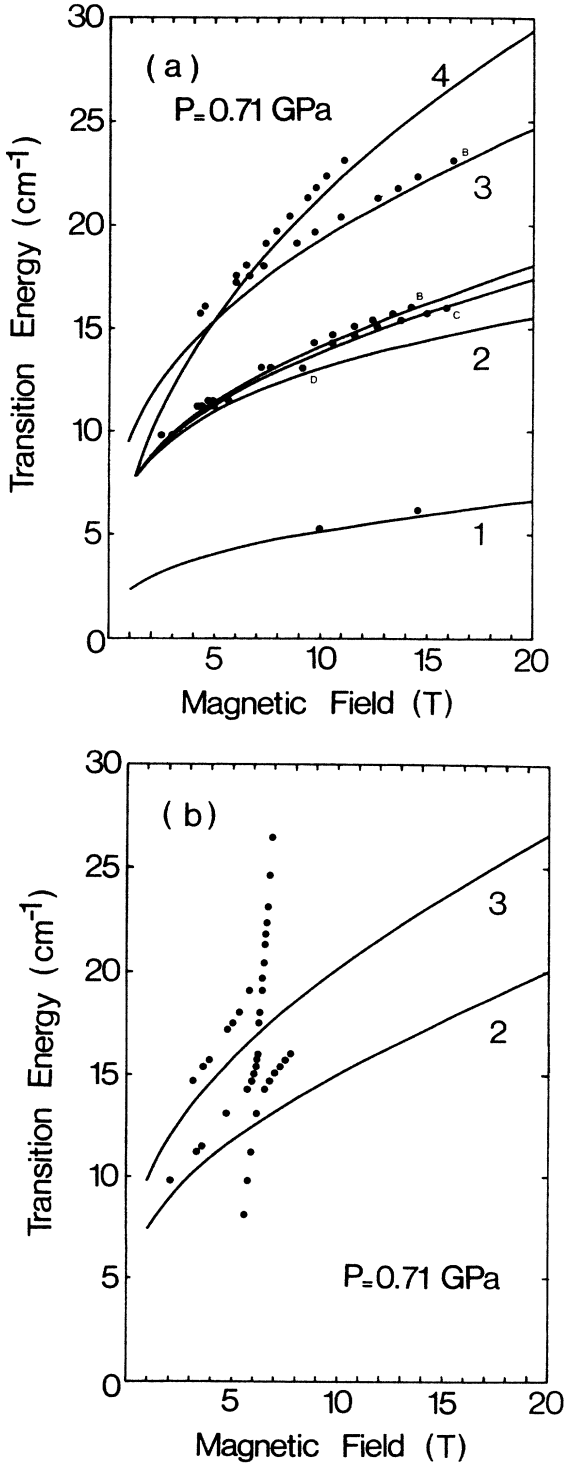

FIG. 10. Same as Fig. 8 but for $P=0.71$ GPa.

position of the peaks, we did change the current to increase the sensitivity of the detection of the weak structures. This allowed us to follow both branches of the anticrossing states of the donor A in a wide energy range, much wider than in FTS experiments.[9]

We now present in Figs. 6–11 the transition energies as a function of the magnetic field for various pressures (Figs. 6–11 are numbered in order of increasing pressure) obtained from the spectra described above. The large number of FIRL lines allows us to follow precisely a given peak as a function of the field and to connect the experimental points with dotted lines as is done in Fig. 6(a) and 6(b) to guide the eye. The comparison with previous experimental results and with the theory permits a unique identification of the transitions. In Figs. 6–11, we can distinguish four different transitions: (1) $(0\bar{1}0)\rightarrow(0\bar{2}0)$; (2) $(000)\rightarrow(0\bar{1}0)$; (3) $(000)\rightarrow(0\bar{2}0)$; (4) $(0\bar{1}0)\rightarrow(0\bar{1}1)$. Transitions (2) and (4) have already been reported and our data are in perfect agreement with previous FTS results.[6,8,9] In Fig. 6 we have also added the experimental points from Ref. 23 for the transition (1). Two of the transitions [(2) and (3)] involve the ground state and are split into up to four components corresponding to the donors A,B,C, and D as shown in Figs. 1–3. Two other transitions [(1) and (4)] are between the excited states. Although transition (1) was observed only for a few FIRL lines (up to three under pressure), the results can be completed by subtraction of the energies of the transitions (3) and (2). This procedure done for the donors A,B, and C gives exactly the same results [shown in Figs. 6(a) and 6(b) by dotted line for transition (1)].

At pressures close to 650 MPa the anticrossing branches for the transitions (2) and (3) involving the donor A were visible. For the sake of clarity we plotted them separately in Figs 8(b), 9(b), and 10(b). Such "interaction" was observed only for the transitions from the $(000)_A$ state [see also transitions $(000)_A\rightarrow(001)$ and $(000)_A\rightarrow(110)$ from Refs. 9 and 10] which indicates that this state is responsible for the observed effects. Figure 12 shows schematically the anticrossing mechanism. The "steep branch" represents the transitions from the deep level of the donor A, i.e., the level determined by the localized portion of the impurity potential. This follows from its energetic position and its pressure and magnetic field dependences (see next section). The slope of the "steep branch" (1.8 meV/T) is simply due to the fact that the final shallow $(0\bar{1}0)$ state involved in the optical transition is very sensitive to the magnetic field while the initial deep state is only slightly sensitive. The observed interaction clearly shows that both the deep and the shallow levels belong to the same center (donor A). The sudden disappearance of all transitions from $(000)_A$ once the deep level becomes populated (see Figs. 2 and 8–11) is also consistent with this picture.[9,10] It is worthwhile to notice that the interaction energy $E_{\min}$ (minimum separation between the two branches) is different on each of the three figures (Figs. 8–10). Since the pressure does not change much from one figure to the other and only the field posi-

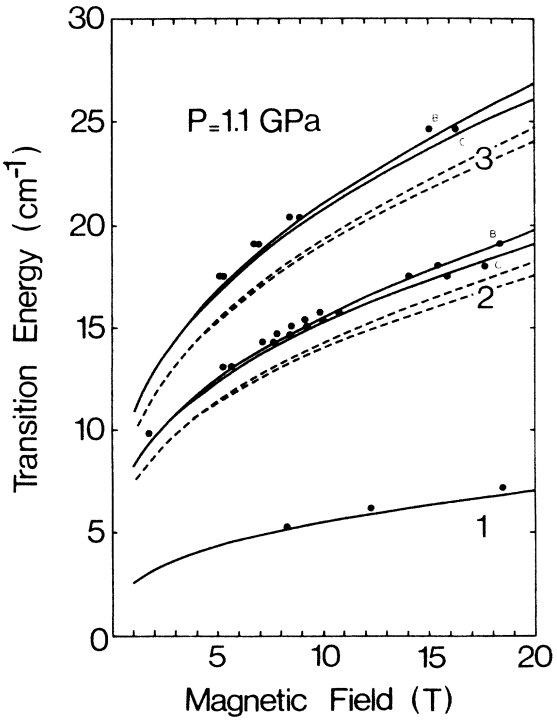

FIG. 11. Same as Fig. 7 but for $P=1.1$ GPa. The donor A is already populated on its deep state so that no more "shallow transitions" for this donor are observed (see the experimental trace of Fig. 2 for the same pressure). Dashed lines were calculated from the TBHB model with the zero-pressure value of $\epsilon_0(\epsilon_0=16.8)$.

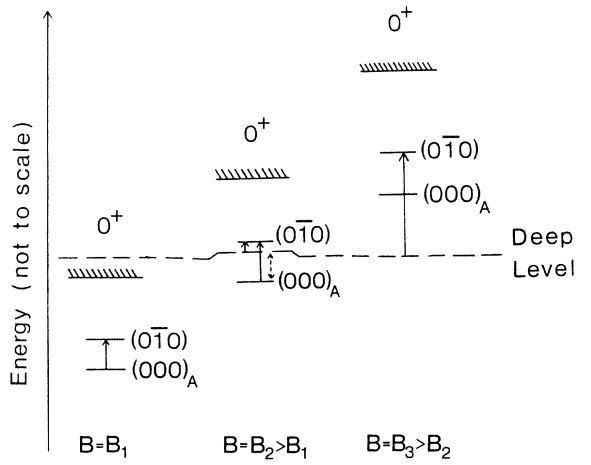

FIG. 12. Schematic of the "anticrossing" mechanism. At a pressure of about 650 MPa the shallow levels connected to the 0^+ Landau level are in a quasiresonant position with the deep level. Sweeping the magnetic field up increases the energy of the $(000)_A$ state while the deep level remains almost unaffected, both states come into resonance $(B=B_2)$. Note that near the anticrossing the deep and the $(000)_A$ states are no longer pure states but a mixture of both (dashed arrow), we still maintain their label for convenience. After the anticrossing the interchange of the states is achieved $(B=B_3)$. At a lower (higher) pressure the anticrossing would occur for a higher (lower) magnetic field. The full arrows indicate optical transitions.

tion of the anticrossing differs significantly, one can expect that the magnetic field and not the pressure is responsible for the change of $E_{\min}$. This will be confirmed in the next section.

IV. QUANTITATIVE DISCUSSION OF THE RESULTS

A. Transitions between shallow donor states

For the theoretical description of our results we used physical parameters of InSb found in the literature without any attempt to adjust them. Band parameters for zero pressure are those of Goodwin and Seiler[24] ($E_g=235.2$ meV, $\Delta=803$ meV, $E_p=23.2$ eV which gives $m^*\sim 0.013\,55 m_0$) which proved to give a very good description of a huge amount of magneto-optical data for InSb. These parameters also very well describe intraconduction band magneto-optical experiments in InSb under pressure[25] with $dE_g/dP=140$ meV/GPa, this value being in very good agreement with direct measurements.[26] Δ and E_p were assumed constant with pressure.[25] The dielectric constant ϵ_0 at $P=0$ was taken from Ref. 27 as 16.8 (which gives $\mathrm{Ry}^*=0.653$ meV) and its pressure dependence as determined in Ref. 28 (see also I).

In Fig. 6(a), we plotted the theoretical curves from the nonparabolic model of I (further denoted as the TBHB model) together with the results of the model of Zawadzki and Wlasak[29] (further denoted as the ZW model). The nonparabolic calculations of Larsen[30] were shown in I to practically coincide with those of TBHB (if the same trial function was used)—therefore we do not display them. In view of some errors in the model of Lin-Chung and Henvis[31] (see I) no attempt was made here to compare it with our results. In Fig. 6(a), both ZW and TBHB theoretical curves were calculated with the adiabatic trial function (double Gaussian of I). As was discussed in I, the adiabatic model is accurate in the high-field limit while in our experiments (especially at high pressures) we may deal with $\gamma\sim 5$. The generalization of the adiabatic model (increasing its accuracy at low fields) which was outlined in I, consists in constructing the donor wave function from several Landau subbands, as was done in Refs. 32 and 33 for the parabolic case. This leads to a system of coupled differential equations. Instead of this rigorous but cumbersome treatment, we propose to improve the nonparabolic variational calculations (both ZW and TBHB) by introducing a correction factor (being a function of γ) for each impurity-level of interest. This factor is determined in the parabolic case as the ratio of the "true" binding energy[33] and the binding energy calculated with the double-Gaussian trial function. This correction factor (given for a few levels and fields in Table I of I) is then used to multiply the energy determined in the nonparabolic approach with the double-Gaussian trial function. Its use in the nonparabolic case is justified by the fact that it is important only in the low-γ region ($\gamma<30$) where the parabolic and nonparabolic models practically coincide (see I).

In Fig. 6(b) all theoretical curves (TBHB and ZW) were calculated with the use of the correction factors. For the transition (1) both models reproduce fairly well the experimental points. For the transitions (2) and (3) the TBHB curves are close to the points of the donor D, thus suggesting that this is the most hydrogeniclike impurity and that all other impurities are characterized by a negative CS (attractive V_{loc}). On the contrary, the ZW curves cross the energies corresponding to donors C and B which implies that the chemical shifts could change their signs at certain fields. Furthermore, the experimental data for the donor A (its strong coupling to the lattice,[34] the interaction between shallow and deep states, an anomalous CS described at the end of this section) strongly suggest that V_{loc} is the largest for this donor. Within the tight-binding approach of Refs. 35 and 36, it turns out that all substitutional donors in InSb should have negative CS, which also confirms the results of TBHB calculations. In view of the tight-binding theory, the impurity Sn has the smallest CS[36] thus our results support the suggestion of Kuchar *et al.*[7] that the residual donor D in InSb might be Sn at an In site. The poor agreement of the ZW curves for the transitions (2) and (3) cannot be removed by any changes of InSb parameters (e.g., ϵ_0) without affecting the good agreement for the transition (1). In Figs. 6(c) and 7–11, we have presented only the TBHB theoretical curves. For the transitions involving the (000) ground state the CS have been included as determined in Eq. (20a) of I with the following values of the $(S\mid V_{\mathrm{loc}}\mid S)$ matrix elements: -0.4, 1.3, 1.9, 3.7×10^3 eV Å^3 for the donors D,C,B, and A, respectively. These values are close to those obtained from pseudopotential calculations for S, Se, and Te donors in InSb.[37]

On Figs. 7–11 good agreement between the theory and the experiment is observed for all transitions except for those involving the ground state of the donor A. Even far from the interaction the "shallow branch" for this donor moves away from the theoretical curves as the pressure is increased. This can be interpreted as the strong pressure variation of $(S\mid V_{\mathrm{loc}}\mid S)$ for the donor A. The CS for this donor achieves at $P\sim 0.6$ GPa the values twice as large as predicted with pressure-independent $(S\mid V_{\mathrm{loc}}\mid S)$. These values are so large that they can no longer be described by the first-order perturbation theory. The strong pressure increase of V_{loc} (Ref. 38) for the donor A may be due to local lattice distortion around this impurity and is consistent with the large lattice-relaxation effects revealed by this donor.[34] The strong pressure variation of the CS was predicted theoretically[39] in the zero-field case (even for the pressure-independent V_{loc}) by summing up all terms of the Wigner-Brillouin perturbation series. The effect which we observe apparently results from both reasons, i.e., the pressure increase of V_{loc} and the breakdown of the first-order perturbation theory.

The transitions from the $(0\bar{1}0)$ state [(1) and (4)] did not reveal any central-cell structure. Moreover, as we already mentioned, the difference of the transition energies (3) and (2) was exactly the same for all four donors. Therefore, up to the experimental accuracy, we did not find any chemical shift for the $(0\bar{1}0)$ state. If, according to pseudopotential calculations of Ref. 37, the matrix elements of $(X\mid V_{\mathrm{loc}}\mid X)$ are of the order of 10^3 eV Å^3 [comparable to $(S\mid V_{\mathrm{loc}}\mid S)$] the formulas from I for the $(0\bar{1}0)$ chemical shifts yield at $B=15$ T the splitting of the $(0\bar{1}0)\rightarrow(0\bar{2}0)$

transitions close to the widths of the observed peaks (see Fig. 4). Therefore, if really $(X \mid V_{\text{loc}} \mid X) \sim 10^3$ eV Å^3 a detailed study of this transition at fields higher than 15 T should reveal the central-cell structure of the peaks.

In Fig. 11, in addition to solid curves calculated for the pressure-dependent ϵ_0 (as determined in Ref. 28) we plotted the dashed lines obtained from TBHB model with pressure-independent $\epsilon_0 = 16.8$. This illustrates the sensitivity of the transition energies to the value of ϵ_0 (and thus to the value of Ry*) and confirms the pressure variation of ϵ_0 given in Ref. 28. It also implies that the $\epsilon_0(P)$ dependence proposed in Ref. 40 was too strong (about twice ours).

Finally, it may be noted that the agreement between the TBHB theory and the experiment would be better if we adopted a slightly higher value of Ry* (this would also modify the chemical shift parameters). However, we preferred not to modify or fit any parameters of InSb. There are still a few sources of inaccuracy of the theory (see I) so that it is not reasonable to demand absolute agreement.

B. Anticrossing of the shallow and deep levels of the donor *A*

Figures 8(b), 9(b), and 10(b) allow for the determination of the slope of the deep-level branch. Both the magnetic field and the pressure dependences of the final states $(0\bar{1}0)$ or $(0\bar{2}0)$ are well described by the TBHB model. We can therefore calculate the field coefficient of the deep level $dE_d/dB = 0.10 \pm 0.10$ meV/T (all coefficients will be given with respect to the Γ_8 valence band at zero field and zero pressure). From Figs. 8(b), 9(b), and 10(b), we can also determine (with high accuracy) the points where the two branches would cross if they did not interact. These three points yield the position of the deep level for the three pressures and thus can be used to calculate $dE_d/dP = 16 \pm 13$ meV/GPa (after taking into account the magnetic field and pressure dependence of the final states as well as the field variation of the deep state given above). This value is in good agreement with recent transport measurements.[12] As opposed to the pressure coefficient of the L-minimum $dE_L/dP \sim 50$ meV/GPa [found in transport measurements in heavily doped n-type InSb (Ref. 41) and confirmed by pseudopotential calculations],[42] it supports our assertion that the observed level is a deep impurity state, with the wave function constructed from the Bloch functions of the whole conduction band (and other bands) and not only from the states of the L-minimum. Obviously, the strongest argument for the deep character of the level is its energetic position far away from any subsidiary minima (at the pressure of 650 MPa, this level lies at least 0.5 eV away from the L-minimum). It is worthwhile to note that the observed interaction implies that both the shallow and the deep states are of the same symmetry.

A theoretical model for the pressure-induced crossing of the impurity levels (for the zero-field case) was introduced by Altarelli and Iadonisi.[43] They considered a Coulombic donor for the conduction band with the absolute minimum at the Γ point of the Brillouin zone and subsidiary minima at X. The anticrossing behavior (interaction) was due to the matrix elements of the Coulomb potential between the Bloch functions of different minima.

In the case which we observed, the model of Altarelli and Iadonisi cannot be applied because of the deep nature of one of the levels. Therefore, we present a simple two-level model of the interaction, taking into account both the Coulombic and the localized portion of the impurity potential as well as the magnetic field terms.

The total Hamiltonian has the form

$$\mathcal{H} = \mathcal{H}_0 + \Delta\mathcal{H}(B) + V_{\text{coul}} + V_{\text{loc}} , \tag{1}$$

where $\mathcal{H}_0$ is the perfect-crystal Hamiltonian, $\Delta\mathcal{H}(B)$ describes the magnetic field part (see I). The shallow state ψ_s is approximately described by the equation

$$[\mathcal{H}_0 + \Delta\mathcal{H}(B) + V_{\text{coul}}]\psi_s = E_s\psi_s , \tag{2}$$

and the localized state ψ_d by

$$(\mathcal{H}_0 + V_{\text{loc}})\psi_d = E_d\psi_d . \tag{3}$$

Here we neglected the Coulomb term and the magnetic field terms relatively small for deep impurities. Now we seek the eigenstates of $\mathcal{H}$ as a combination of ψ_s and ψ_d:

$$\psi = \alpha_s\psi_s + \alpha_d\psi_d . \tag{4}$$

Inserting it into $\mathcal{H}\psi = E\psi$, multiplying by $\int \psi_s^*$ and $\int \psi_d^*$ we obtain the secular equation for the energies

$$\begin{vmatrix} \mathcal{H}_{ss} - E & \mathcal{H}_{sd} - EC \\ \mathcal{H}_{ds} - EC^* & \mathcal{H}_{dd} - E \end{vmatrix} = 0 , \tag{5}$$

where $C = (\psi_s \mid \psi_d) \ll 1$ (as the two functions have different localizations both in $\mathbf{r}$ and $\mathbf{k}$ spaces), and

$$\mathcal{H}_{ss} = E_s + (\psi_s \mid V_{\text{loc}} \mid \psi_s) , \tag{6a}$$

$$\mathcal{H}_{dd} = E_d + [\psi_d \mid \Delta\mathcal{H}(B) \mid \psi_d] + (\psi_d \mid V_{\text{coul}} \mid \psi_d) . \tag{6b}$$

The corrected values of the energies $\mathcal{H}_{ss}$ and $\mathcal{H}_{dd}$ may be taken from the experiment. The off-diagonal part in (5) which leads to the interaction may be written as

$$\mathcal{H}_{sd} - EC \cong (E_s + E_d - E_0 - E)\Phi_s(\mathbf{0})(S \mid \psi_d) , \tag{6c}$$

where we used the one-band effective-mass approximation for $\psi_s = \Phi_s \mid S)[\mid S)$ being the Bloch function at $\mathbf{k} = 0, \mathcal{H}_0 \mid S) = E_0 \mid S,]$ and the strong localization of $\psi_d(\mathbf{r})$ compared with $\Phi_s(\mathbf{r})$. The minimum separation between the two interacting branches can then be obtained from Eq. (5):

$$E_{\min} \cong 2 \mid (E_s + E_d - E_0 - E)\Phi_s(\mathbf{0})(S \mid \psi_d) \mid . \tag{7}$$

In Fig. 13, we plot the experimental values of $E_{\min}$ versus the value of the shallow-state envelope function at the donor site $|\Phi_s(\mathbf{0})|$ calculated from the TBHB model with the double-Gaussian trial function. The proportionality is clearly visible. This implies that in Eq. (7) the quantity $(E_s + E_d - E_0 - E)$ does not change with the magnetic field [$(S \mid \psi_d)$ is field independent]. However,

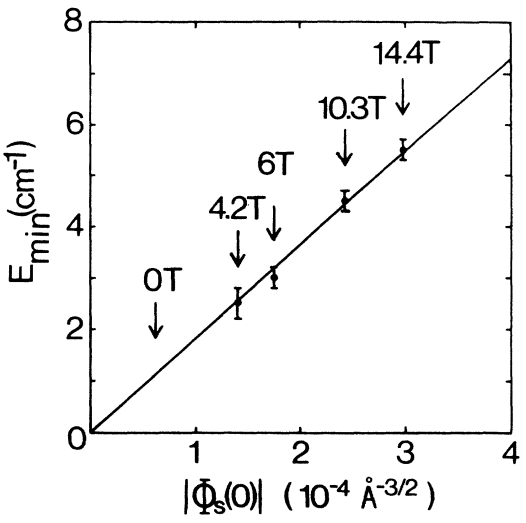

FIG. 13. Minimum separation between the two interacting branches [see Figs. 8(b), 9(b), and 10(b)] versus the value of the (000) state envelope function at the impurity site, $|\Phi_s(0)|$. $\Phi_s(0)$ was calculated from the TBHB model at the values of the magnetic field and pressure at which the crossover would occur.

the shallow-state energy relative to the Γ minimum, $E_s - E_0$, changes from 5 to 20 meV in the range of the experimental points of Fig. 13. Therefore, we can state that the Coulombic potential contribution $E_d - E$ to the energy of the deep state must be considerable (the magnetic field contribution to its energy is negligible as follows from the theoretical considerations of Ref. 44 and the estimated value of dE_d/dB). The above conclusion agrees with that of Ref. 45 that the Coulombic potential contribution to the energy of highly localized states is of the order of 100 meV.

Adopting this value as an estimate of the energy difference in Eq. (7) we obtain $(S \mid \psi_d)/\sqrt{\Omega_0} \sim 1.6$ [this gives $(\psi_s \mid \psi_d) \sim 10^{-3}$ at the field of 10 T]. Such value is consistent with the localized character of the considered state, e.g., for ψ_d being a Wannier function (sum of the Bloch functions from the whole conduction band) we would get $(S \mid \psi_d)/\sqrt{\Omega_0} = 1$.

The simplest description of the highly localized impurity state can be made within the one site—one band Koster-Slater model.[46] Following the approach developed in Ref. 47 for InSb:S,Se we obtained $(S \mid \psi_d)/\sqrt{\Omega_0}$ about 3 times larger than the above estimated value. On the other hand, the Koster-Slater model yields the $(S \mid V_{loc} \mid S)$ matrix element over an order of magnitude smaller than the one deduced from our experimental values of the chemical shifts for the donor A. This implies that the simple one site—one band model is not adequate to describe the properties of the observed deep state.

The two-level model described above enables us to calculate the matrix elements for the optical transitions to the excited states of donor A. This can be compared with the experimentally observed intensities of the lines and good agreement is obtained.[10]

V. SUMMARY AND CONCLUSIONS

The transitions between the excited states [(1) and (4)] shown in Figs. 6—11 are very well reproduced by the TBHB calculations both at zero and at high pressure provided that the pressure dependence of ϵ_0 is taken into account. Within the experimental accuracy we do not observe the chemical shift for the $(0\bar{1}0)$ state, possible in the nonparabolic TBHB model. The comparison of the theory and the experiment for the transitions involving the ground state [(2) and (3)] reveals that the donor D is the most hydrogeniclike. All other donors possess negative chemical shifts, consistent with the tight-binding theory predictions.[36] The matrix elements $(S \mid V_{loc} \mid S)$ for the donors B,C, and D (obtained from the chemical shifts) remained constant with pressure and field and their values were close to those obtained in pseudopotential calculations[37] and transport measurements. On the contrary, the chemical shift for the donor A increased anomalously with pressure, indicating that the localized part of the impurity potential for this donor strongly depends on the pressure. This seems reasonable in view of the large-lattice-relaxation effects observed for another deep state of this impurity.[9,34]

At the pressures around 0.65 GPa our results reveal the interaction between two levels of the donor A, reported previously in Ref. 9. The deep character of one of these levels, which follows from its energetic position, is also confirmed by its pressure coefficient and the observed features of its wave function. These features, together with the estimation of the Coulomb-potential effect on the deep state, were determined from the analysis of the interaction energy. The rapid change of localization of the ground state during the anticrossing should manifest itself in the experiments like ESR or ENDOR, which yield the value of the wave function at the impurity site. The observed interaction is also a challenge for the theoretical models of impurity states as both parts of the potential (i.e., Coulombic and localized) should be considered simultaneously.

ACKNOWLEDGMENTS

It is a pleasure to acknowledge stimulating discussions with Professor S. Porowski, Professor J. C. Portal, and Professor J. L. Robert, and with Dr. R. Aulombard, Dr. G. Martinez, and Dr. Z. Wasilewski. We thank Dr. L. Dmowski for assistance during some experiments. Two of us (M.B. and W.T.) have the pleasure to acknowledge the financial support they received from the Université Scientifique et Médicale de Grenoble during their stay in Grenoble. The Service National des Champs Intenses is "Laboratoire associé à l'Université Scientifique et Médicale de Grenoble" and "Laboratoire propre No. 5021 du Centre National de la Recherche Scientifique."

*On leave of absence from the Institute of Experimental Physics, Warsaw University, Hoza 69, PL-00-681 Warsaw, Poland.

†On leave of absence from the High Pressure Research Center (UNIPRESS), Polish Academy of Sciences, Sokolowska 29, PL-01-142 Warsaw, Poland.

[1]W. Trzeciakowski, M. Baj, S. Huant, and L. C. Brunel, Phys. Rev. B **33**, 6846 (1986).

[2]R. Kaplan, J. Phys. Soc. Jpn. Suppl. **21**, 249 (1966).

[3]R. Kaplan, Phys. Rev. **181**, 1154 (1969).

[4]R. Kaplan, in *Proceedings of the International Summer School on Narrow Gap Semiconductors, Nimes, 1979,* edited by W. Zawadzki (Springer, Berlin, 1980), p. 138.

[5]R. A. Cooke, Ph.D. thesis, University of Oxford, 1979.

[6]R. Kaplan, R. A. Cooke, and R. A. Stradling, Solid State Commun. **26**, 741 (1978).

[7]F. Kuchar, R. Kaplan, R. J. Wagner, R. A. Cooke, R. A. Stradling and P. Vogl, J. Phys. C **17**, 6403 (1984).

[8]A. M. Davidson, P. Knowles, S. Porowski, R. A. Stradling and Z. Wasilewski, in *Proceedings of the Oji International Seminar on the Physics in High Magnetic Fields, Hakone, 1980,* edited by S. Chikazumi and M. Miura (Springer, Berlin, 1981), p. 84.

[9]Z. Wasilewski, A. M. Davidson, R. A. Stradling, and S. Porowski, in *Proceedings of the Sixteenth International Conference on the Physics of the Semiconductors, Montpellier, 1982,* edited by M. Averous (North-Holland, Amsterdam, 1983), p. 89; in *Proceedings of the International Conference on the Application of High Magnetic Fields in Semiconductor Physics, Grenoble, 1982,* edited by G. Landwehr (Springer, Berlin, 1983), p. 233.

[10]Z. Wasilewski, R. A. Stradling, M. Baj, L. C. Brunel, S. Huant, W. Trzeciakowski, and S. Porowski, Acta Phys. Polonica A **67**, 405 (1985).

[11]M. Konczykowski, S. Porowski, and J. Chroboczek, in *Proceedings of the Eleventh International Conference of the Physics of Semiconductors, Warsaw, 1972,* (Polish Scientific, Warsaw, 1972), p. 1050.

[12]R. Piotrzkowski (private communication).

[13]W. Paul, in *Proceedings of the Ninth International Conference on the Physics of Semiconductors, Moscow, 1968* (Nauka, Leningrad, 1968), p. 16.

[14]W. Jantsch, K. Wünstel, O. Kumagai, and P. Vogl, Phys. Rev. B **25**, 5515 (1982).

[15]Preliminary results were presented by M. Baj, L. C. Brunel, S. Huant, W. Trzeciakowski, Z. Wasilewski, and R. A. Stradling, in *Proceedings of the Seventeenth International Conference on Physics of Semiconductors, San Francisco, 1984,* edited by D. J. Chadi (Springer, New York, 1985), p. 667.

[16]S. Huant, L. C. Brunel, M. Baj, L. Dmowski, N. Coron, and G. Dambier, Solid State Commun **54**, 131 (1985).

[17]N. Coron, G. Dambier, J. Leblanc, and J. P. Moalic, Rev. Sci. Instrum. **46**, 492 (1975).

[18]Z. Wasilewski, S. Porowski, and R. A. Stradling, J. Phys. E (to be published).

[19]M. Konczykowski, M. Baj, E. Szafarkiewicz, L. Konczewicz, and S. Porowski, in *Proceedings of the International Conference on High Pressure and Low Temperature Physics, Cleveland, 1977,* edited by C. W. Chu and J. A. Woolam (Plenum, New York, 1978), p. 523.

[20]P. E. Simmonds, J. M. Chamberlain, R. A. Hoult, R. A. Stradling, and C. C. Bradley, J. Phys. C **7**, 4164 (1974).

[21]For a recent review of the magnetic freeze-out problem in InSb, see for instance A. Raymond, in *Proceedings of the International Conference on the Application of High Magnetic Fields in Semiconductor Physics, Grenoble, 1982,* edited by G. Landwehr (Springer, Berlin, 1983), p. 344.

[22]The effect of such terms on the selection rules has been recently considered by J. Wlasak, Acta Phys. Polonica (to be published).

[23]L. E. Blagosklonkaya, E. M. Gershenzou, G. N. Goltsman, and A. I. Elantev, Fiz. Tekh. Poluprov. Odn. **11**, 2373 (1977) [Sov. Phys. Semicond. **11**, 1395 (1977)].

[24]M. W. Goodwin and D. G. Seiler, Phys. Rev. B **27**, 3451 (1983).

[25]S. Huant, L. Dmowski, M. Baj, and L. C. Brunel, Phys. Status Solidi B **125**, 215 (1984); S. Huant, Thèse de troisième cycle, University of Grenoble, 1984 (unpublished).

[26]N. Menuyk, A. S. Pine, J. A. Kafalas, and A. J. Strauss, J. Appl. Phys. **45**, 3477 (1974).

[27]J. R. Dixon and J. K. Furdyna, Solid State Commun. **35**, 195 (1980).

[28]W. Trzeciakowski and M. Baj, Solid State Commun. **52**, 669 (1984).

[29]W. Zawadzki and J. Wlasak, in *Theoretical Aspects and New Developments in Magneto-optics,* edited by J. T. Devreese (Plenum, New York, 1980), p. 347.

[30]D. M. Larsen, J. Phys. Chem. Solids, **29**, 271 (1968).

[31]P. J. Lin Chung and B. W. Henvis, Phys. Rev. B **12**, 630 (1975).

[32]J. Simola and J. Virtamo, J. Phys. B **11**, 3309 (1978).

[33]W. Rösner, G. Wunner, H. Herold, and H. Ruder, J. Phys. B **17**, 29 (1984).

[34]L. Dmowski, M. Baj, P. Ioannides, and R. Piotrzkowski, Phys. Rev. B **26**, 4495 (1982).

[35]H. P. Hjalmarson, P. Vogl, D. J. Wolford, and J. D. Dow, Phys. Rev. Lett. **44**, 810 (1980).

[36]P. Vogl, in *Festkörperprobleme,* Vol. 21 of *Advances in Solid State Physics,* edited by J. Treusch (Vieweg, Braunschweig, 1981), p. 191.

[37]I. Gorczyca, Phys. Status Solidi B **103**, 529 (1981).

[38]The pressure variation of the Bloch function is negligible according to Gorczyca (Ref. 42) and also in view of our results for the chemical shifts of all the other donors.

[39]W. Trzeciakowski and J. Krupski, Solid State Commun. **44**, 1491 (1982).

[40]W. Zawadzki and J. Wlasak, J. Phys. C **17**, 2505 (1984).

[41]L. Konczewicz, E. Litwin-Staszewska, and S. Porowski, in *Proceedings of the Third International Conference on the Physics of Narrow Gap Semiconductors, Warsaw, 1977,* edited by J. Rauluszkiewicz, M. Gorska, and E. Kaczmarek (Polish Scientific, Warsaw, 1978), p. 211.

[42]I. Gorczyca, Phys. Status Solidi B **112**, 97 (1982).

[43]M. Altarelli and G. Iadonisi, Nuovo Cimento **5B**, 21 (1971).

[44]W. Pötz and P. Vogl, Solid State Commun. **48**, 249 (1983).

[45]C. O. Rodriguez, S. Brand, and M. Jaros, J. Phys. C **13**, L333 (1980).

[46]J. Callaway, *Quantum Theory of the Solid State* (Academic, New York, 1974), part II.

[47]L. Konczewicz and W. Trzeciakowski, Phys. Status Solidi B **115**, 359 (1983).